

Preparation of hyaluronic acid-coated polymeric micelles for nasal vaccine delivery

Kengo Suzuki,^a Yuta Yoshizaki,^{†b} Kenta Horii,^a Nobuo Murase,^b Akinori Kuzuya,^{a,c} Yuichi Ohya*^{a,d}

Received 00th January 20xx,
Accepted 00th January 20xx

DOI: 10.1039/x0xx00000x

Hyaluronic acid (HA)-coated biodegradable polymeric micelles were developed as nanoparticulate vaccine delivery systems to establish an effective nasal vaccine. We previously reported HA-coated micelles prepared by forming a polyion complex (PIC) of poly(L-lysine)-*b*-polylactide (PLys⁺-*b*-PLA) micelles and HA. The HA-coated micelles exhibited specific accumulation in HA receptor-expressing cells and extremely high colloidal stability under diluted blood conditions. In this study, a model antigen, ovalbumin (OVA), and an adjuvant oligonucleotide containing the CG motif (CpG-DNA) were efficiently loaded in HA-coated micelles *via* electrostatic interactions. HA-coated micelles delivered OVA and CpG-DNA in mouse bone marrow-derived dendritic cells (BMDCs) and resulted in upregulation of mRNA encoding IFN- γ and IL-4 in BMDCs. In addition, HA-coated micelles enhanced the expression of the major histocompatibility complex (MHC) class II on BMDCs. We investigated the immune response of HA-coated micelles following intranasal administration. HA-coated micelles induced higher OVA-specific IgG in the blood and OVA-specific IgA in the nasal wash than control (carboxymethyl dextran-coated) micelles. These results suggest that HA-coated micelles efficiently deliver antigens and adjuvants to mucosal-resident immune cells. Therefore, HA-coated micelles are promising platforms for developing nasal vaccines against infectious diseases.

Introduction

Vaccines provide immunity to prevent infectious diseases. Recently developed mRNA vaccines for severe acute respiratory syndrome coronavirus 2 (SARS-CoV2) have succeeded in exhibiting preventive effects and reducing the risk of severe disease¹. Usually, these vaccines are administered either subcutaneously or intramuscularly. They are then taken up by antigen-presenting cells such as dendritic cells (DCs) to induce systemic immunity². However, vaccination for a pandemic outbreak of infectious diseases requires significant labour from medical care workers. Therefore, simplified administration methods and dosage reduction are highly desired. The nasal administration route requires no injection needles and allows applicants to self-vaccinate themselves. Furthermore, intranasal immunisation can induce IgA production, which plays a major role in the mucosal immune response³. Therefore, nasal vaccines are suitable for preventing viruses such as coronaviruses from invading the upper respiratory tract⁴. This strategy has already been used for the influenza vaccine^{5–10}.

The mucosa is the frontline of contact with the exterior of the body. Hence, foreign substances are quickly eliminated from the mucosa owing to the barrier provided by mucosal epithelial cells and the continuous substantial secretion of

mucus¹¹. As antigen-presenting cells such as DCs are located under the mucosal epithelium¹², it is crucial to develop an efficient vaccine carrier that can pass through the mucosal tissue.

Nanoparticle vaccines may improve the safety and efficacy of vaccine administration, reduce the administration frequency, and simplify the administration method^{13–17}. In addition, from the viewpoint of antigen protection from proteolysis, and efficient delivery to cells, nanoparticles are excellent carriers for drug delivery systems¹⁸. Therefore, vaccination *via* the use of nanoparticles in the nasal mucosa is attracting attention as a minimally invasive vaccination method. In particular, hyaluronic acid (HA)-modified nanoparticles have been studied as carriers for nasal vaccines owing to the expression of HA receptors (such as CD44) by the mucosal epithelium and DCs^{19–21}. Verheul *et al.* reported the preparation of covalently stabilised nanoparticles of thiolated trimethylchitosan and thiolated HA for nasal and intradermal vaccines²². As a result, the immunogenicity of the antigen in the vaccine was improved in both the nose and the skin. Liu *et al.* prepared HA-modified hybrid nanoparticles consisting of poly(lactide-*co*-glycolic acid) (PLGA) as effective vaccine carriers by electrostatic interactions²³. Their study revealed that the nanoparticles improved the stability and biocompatibility and induced robust humoral immunity by active targeting using CD44-expressing DCs. In addition, esterified or thiolated HAs have been developed to modify the surface of polymeric micelles with poly(ethylene glycol)^{24,25}. These HA-modified micelles were evaluated for their application as transmucosal delivery carriers. However, it is known that the modification of the carboxyl group of HA reduces the mucosal adhesion property as the hydrogen bonds of the carboxyl group promote the mucosal adhesion property^{26,27}.

^a Faculty of Chemistry, Materials, and Bioengineering, Kansai University, 3–3–35 Yamate, Suita, Osaka 564–8680, Japan

^b Organization for Research and Development of Innovative Science and Technology (ORDIST), Kansai University, 3–3–35 Yamate, Suita, Osaka 564–8680, Japan

^c Kansai University Medical Polymer Research Center (KUMP-RC), Kansai University, 3–3–35 Yamate, Suita, Osaka 564–8680, Japan

[†] Present address: Graduate School of Pharmaceutical Sciences, Tohoku University, 6–3 Aoba, Aramaki, Aoba-ku, Sendai, Miyagi 980–8578, Japan
Electronic Supplementary Information (ESI) available: [details of any supplementary information available should be included here]. See DOI: 10.1039/x0xx00000x

Moreover, researches on drug delivery by polymeric micelles using amphiphilic block polymers have also been actively carried out^{28–32}. In particular, there are many reports on polymeric micelles utilising electrostatic interactions, such as PIC formation. For example, Fan *et al.* investigated the co-assembly of positively charged patchy micelles and negatively charged bovine serum albumin molecules³³. Patchy micelles are prepared using block copolymer brushes as templates, leading to the co-assembly of protein molecules into vesicular structures. Min *et al.* prepared antibody fragment (Fab)-installed PIC micelles and reported the delivery of the interfering RNA (siRNA) to pancreatic cancer cells³⁴. In another study, Wang *et al.* prepared self-assembled stable micelles with polyion-stabilised cores, consisting of a mixture of methoxy PEG-PDLLA-polyglutamate and methoxy PEG-PDLLA-poly(L-lysine). They reported that the interaction of anionic and cationic charged polyionic segments could be an effective strategy for controlling drug release and improving the stability of polymer-based nanocarriers³⁵.

In a previous study^{36,37}, we successfully prepared positively charged biodegradable polymeric micelles composed of AB block copolymers of poly(L-lysine) and polylactide (PLys⁺-*b*-PLLA). Furthermore, we reported HA-coated micelles synthesis by forming a polyion complex (PIC) of positively charged PLys⁺-*b*-PLLA micelles with HA, a negatively charged polysaccharide. The HA-coated micelles exhibited superior colloidal stability, excellent stability against dilution, and a high affinity for liver sinusoidal epithelial cells (LSECs)^{36,37}.

HA exhibits mucosal adhesion owing to its high hydration ability. In addition, HA receptors are expressed in immune cells such as DCs, macrophages, and mucosal epithelial cells. Therefore, HA-coated micelles can be used as target-oriented materials. Antigen proteins with negative charges and an anionic nucleic acid derivative with adjuvant activity can bind

to the positively charged PLys⁺-*b*-PLLA micelles on the surface via electrostatic interactions. Furthermore, efficient delivery of nanoparticles to immunocompetent cells, such as DCs, can be expected by coating the micelles with HA. Such a vaccine system may lead to the development of a nasal vaccine that can be administrated *via* the nasal mucosa.

In this study, we designed HA-coated micelles containing antigens and adjuvants. Ovalbumin (OVA) was used as a model antigen. An oligonucleotide containing the CG motif (CpG-DNA) was used as an adjuvant to act as a synthetic ligand for Toll-like receptor 9 and to activate DCs^{38,39}. As OVA (isoelectric point (pI) = 4.6) and CpG-DNA are anionic molecules, they are expected to attach to positively charged PLys⁺-*b*-PLLA micelles *via* electrostatic interactions. Further coating with anionic HA produced an HA-coated micellar vaccine (Fig. 1). We investigated the delivery function to immune cells and the ability to induce humoral immunity and antigen-specific antibody levels in mice.

Results and discussion

Preparation of HA-coated micelles containing OVA and CpG-DNA

Synthesis of PLys⁺-*b*-PLLA was carried out according to previous reports^{29,30}. The details are shown in the ESI. As a result of the synthesis, PLys⁺-*b*-PLLA with a degree of polymerisation of PLYS segment 28 and PLLA segment 22 were obtained. Positively charged PLys⁺-*b*-PLLA micelles were prepared using the solvent evaporation method according to a previous report³⁷. Dynamic light scattering (DLS) measurements revealed that the obtained PLys⁺-*b*-PLLA micelles had an average micelle size of 69 nm (polydispersity index (PDI): 0.25) (Fig. 2A) and a zeta potential of +22 mV. Transmission electron microscopy (TEM) analysis of the micelles also demonstrated that their diameters were in the range of 40–60 nm (Fig. 2B). HA-coated micelles were obtained by PIC formation of positively charged PLys⁺-*b*-PLLA micelles and negatively charged HA³⁷. We obtained HA-coated micelles containing rhodamine B-labelled OVA and FAM(fluorescein)-labelled CpG-DNA (HA-micelle(OC)) by treating PLys⁺-*b*-PLLA micelles with a solution containing negatively charged OVA (antigen) and CpG-DNA (adjuvant). DLS measurements estimated the average micelle size to be 157 nm (PDI: 0.19) (Fig. 2A) and calculated a zeta potential of –21 mV. We also confirmed by TEM observation that the HA-micelle(OC) size was approximately 100–120 nm (Fig. 2B). The size of the HA-micelle(OC) was larger than that of the PLys⁺-*b*-PLLA micelles. In addition, from PLys⁺-*b*-PLLA micelles to HA-micelle(OC), the zeta potential changed from positive to negative. These results indicated a successful coating of HA on PLys⁺-*b*-PLLA micelles. In addition, the fluorescence measurements after treatment with Triton X-100 estimated 80.5 and 79.7% entrapment efficiency (%) of rhodamine B-labelled OVA and FAM-labelled CpG-DNA, respectively. The following equation was used to calculate the efficiency:

$$\text{Entrapment efficiency (\%)} = \frac{\text{OVA (or CpG-DNA) loaded (\%)} \text{ found}}{\text{OVA (or CpG-DNA) loaded (\%)} \text{ in feed}} \times 100$$

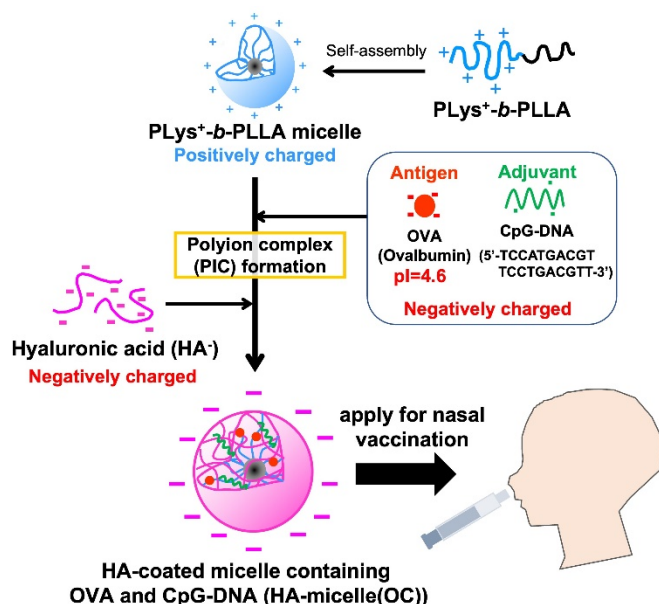


Fig. 1. Schematic illustration of nasal vaccine delivery system using HA-coated micelles containing OVA as an antigen and CpG-DNA as an adjuvant.

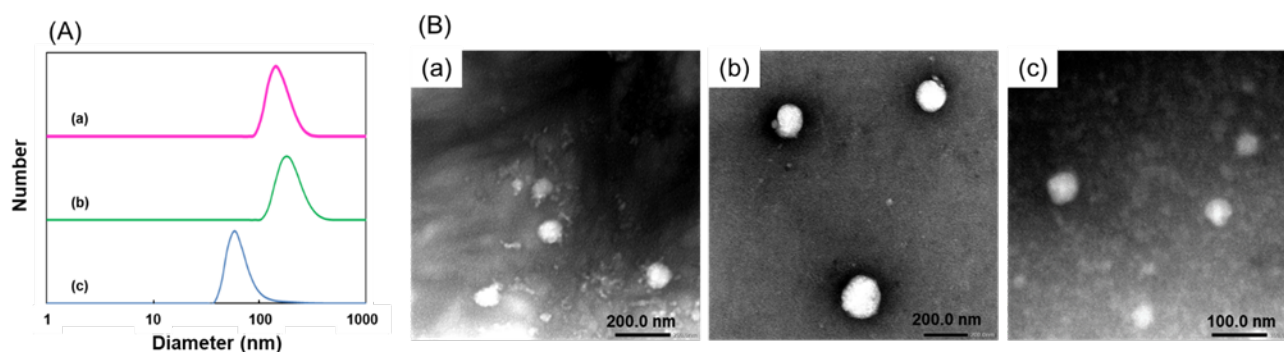


Fig. 2. (A) Size distribution of (a) HA-micelle(OC), (b) Dex-micelle(OC) and (c) PLYS⁺-b-PLLA micelle measured by DLS. (B) TEM images for (a) HA-micelle(OC), (b) Dex-micelle(OC) and (c) PLYS⁺-b-PLLA micelle.

In addition, we prepared carboxymethyl dextran (CM-Dex)-coated micelles containing rhodamine B-labelled OVA and FAM-labelled CpG-DNA, Dex-micelle(OC), as control samples. CM-Dex is used as an anionic polysaccharide, for which mucosal epithelial cells and immune cells do not possess specific receptors. The average micelle size of Dex-micelle(OC) and the zeta potential were 198 nm (PDI: 0.22) and -18 mV, respectively (Fig. 2A). Furthermore, the micelle size observed in the TEM images was approximately 100–150 nm (Fig. 2B), suggesting that Dex-micelle(OC) have slightly larger diameters compared to the HA-micelle(OC). The entrapment efficiencies of rhodamine B-labelled OVA and FAM-labelled CpG-DNA were 92.8 and 83.0%, respectively. HA-micelle(OC) and Dex-micelle(OC) containing non-labelled-OVA and CpG-DNA were also prepared and used for determination of MHC class II molecules expression on BMDCs and *in vivo* experiments.

Uptake of HA-micelle(OC) into BMDCs

We investigated the uptake behaviour of HA-micelle(OC) into BMDCs using a confocal laser scanning microscope (CLSM). Both red fluorescence from rhodamine-labelled OVA (excitation at 561 nm) and green fluorescence from FAM-labelled CpG-DNA (excitation 488 nm) were observed in BMDCs incubated with HA-micelle(OC) (Fig. 3 (a-c)). On the other hand, almost no fluorescence was observed when cells were incubated with an aqueous solution of rhodamine-labelled OVA and FAM-labelled CpG-DNA (Figure 3 (d-e)). In the merged image (Figure 3 (c)), almost only a yellow colour (overlapped green and red) was observed in the BMDCs treated with HA-micelle(OC). These results indicate that OVA and CpG-DNA were accumulated at the same location in the cells, and the HA-micelle(OC) did not decompose during the incubation time.

Quantitative estimation of the population of BMDCs uptake of HA-micelle(OC) was analysed by Flow cytometric analysis (FCA) (Fig. 4). A slight increase in the fluorescence intensity of BMDCs treated with a solution of rhodamine-labelled OVA and FAM-labelled CpG-DNA was observed compared to those treated with PBS(-) (autofluorescence). However, a significantly higher population of cells with stronger fluorescence was observed in BMDCs treated with HA-micelle(OC). Results of

FCM for Dex-micelle(OC) are attached as Figure S6 in ESI. Although slight uptake of Dex-micelle(OC) into BMDC was observed, the amount of the uptake was smaller than HA-micelle(OC). This result is consistent with the results of the CLSM observation and indicates that the uptake of OVA and CpG-DNA into BMDCs could be significantly enhanced using HA-micelle(OC).

Activation of BMDC by HA-micelle(OC)

The expression of mRNA encoding cytokines (IFN- γ and IL-4) was investigated by quantitative reverse transcription polymerase chain reaction (RT-qPCR) to estimate the activation behaviour of BMDCs by HA-micelle(OC) (Fig. 5). When treated with HA-micelle(OC), the expression levels of both cytokines (IFN- γ and IL-4) were significantly increased compared to those treated with intact HA-micelle (without OVA and CpG-DNA), and the aqueous solution of OVA and CpG-DNA. The increase in cytokine mRNA expression suggested that CpG-DNA was effectively delivered to BMDCs by HA-micelle(OC) and stimulated to induce the maturation of BMDCs. Moreover, the expression of MHC class II in BMDCs was investigated using FCA (Fig. 6 and Fig. S5). MHC class II plays an essential role in priming helper T cells to induce cellular and humoral immunities. Significantly higher expression of MHC class II molecules on the cells was observed in BMDCs treated with HA-micelle(OC) compared with BMDCs treated with a solution of OVA and CpG-DNA. These results suggest that HA-micelle(OC) efficiently delivered antigen (OVA) and adjuvant (CpG-DNA) to BMDCs and activated the cells.

In vivo immunological response by nasal administration of HA-micelle(OC)

Finally, we investigated the *in vivo* immunological response to nasal administration of HA-micelle(OC). After administration of HA-micelle(OC) to mice via the nasal route, OVA-specific IgG antibody titer in serum and OVA-specific IgA antibody titer in saliva and nasal lavage fluid were determined by enzyme-linked immunosorbent assay (ELISA). Dex-micelle(OC) were used as a control in these experiments.

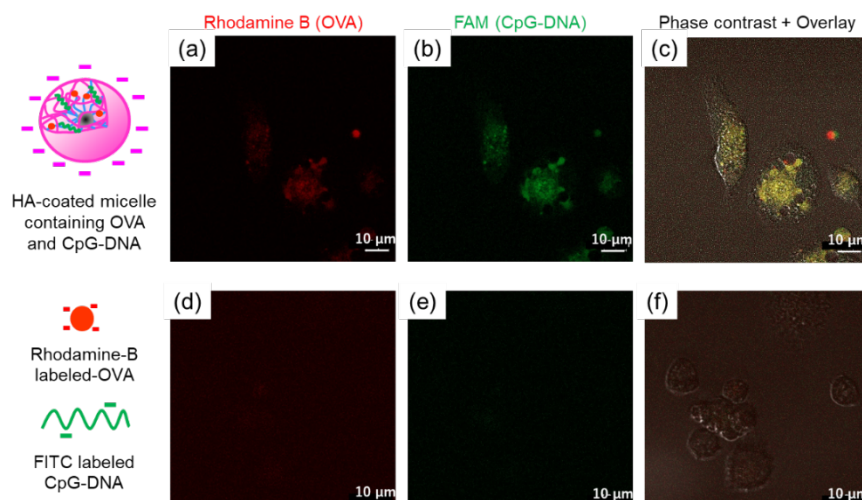


Fig. 3. Confocal laser scanning microscopic images of BMDCs incubated with HA-micelle(OC) (a, b, and c) or aqueous solution Rhodamine-labelled OVA and FAM-labelled CpG-DNA (d, e, and f) at 37°C for 4 h in the presence of 5% FBS contained RPMI-1640. (a) and (d) rhodamine B, (b) and (e) FAM(FITC), (c) and (f) phase contrast image + overlay.

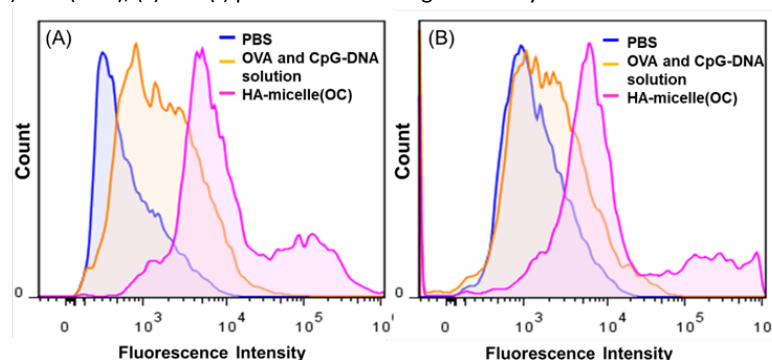


Fig. 4. Flow cytometric analysis (FCA) for BMDCs incubated with HA-micelle(OC) or aqueous solution Rhodamine-labelled OVA and FAM-labelled CpG-DNA at 37°C for 4 h. (A) Rhodamine B detection (OVA), (B) FAM detection (CpG-DNA).

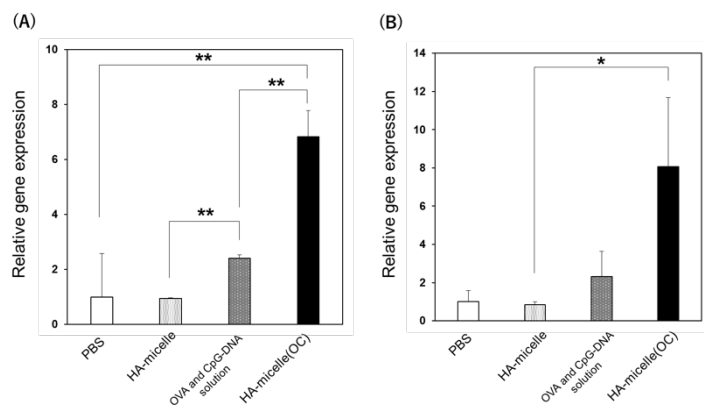


Fig. 5. Relative mRNA expression of IFN- γ (A) and IL-4 (B) toward housekeeping gene (β -Actin) in BMDCs measured by RT-qPCR. Cells were incubated with HA-micelle(OC), aqueous solution of OVA and CpG-DNA, intact HA-micelle (without OVA and CpG-DNA) or PBS at 37°C for 24 h in the presence of serum. Data represent mean \pm SD ($n = 3-5$). * $P < 0.05$, ** $P < 0.01$

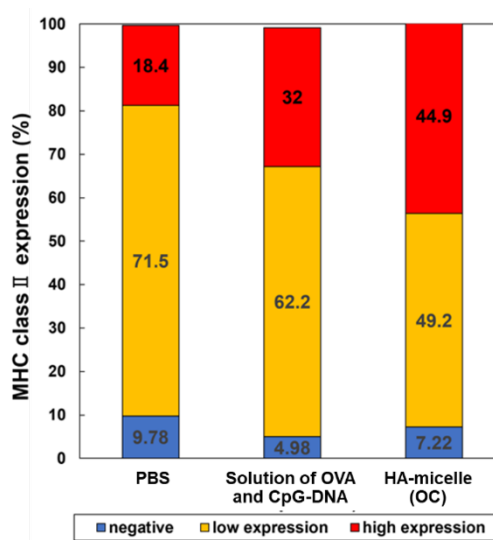


Fig. 6. Expression of MHC class II in BMDCs incubated with HA-micelle(OC), aqueous solution of OVA and CpG-DNA or PBS. Cells were incubated with HA-micelle(OC), an aqueous solution of OVA and CpG-DNA or PBS in RPMI-1640 containing 5% FBS for 24 h at 37°C.

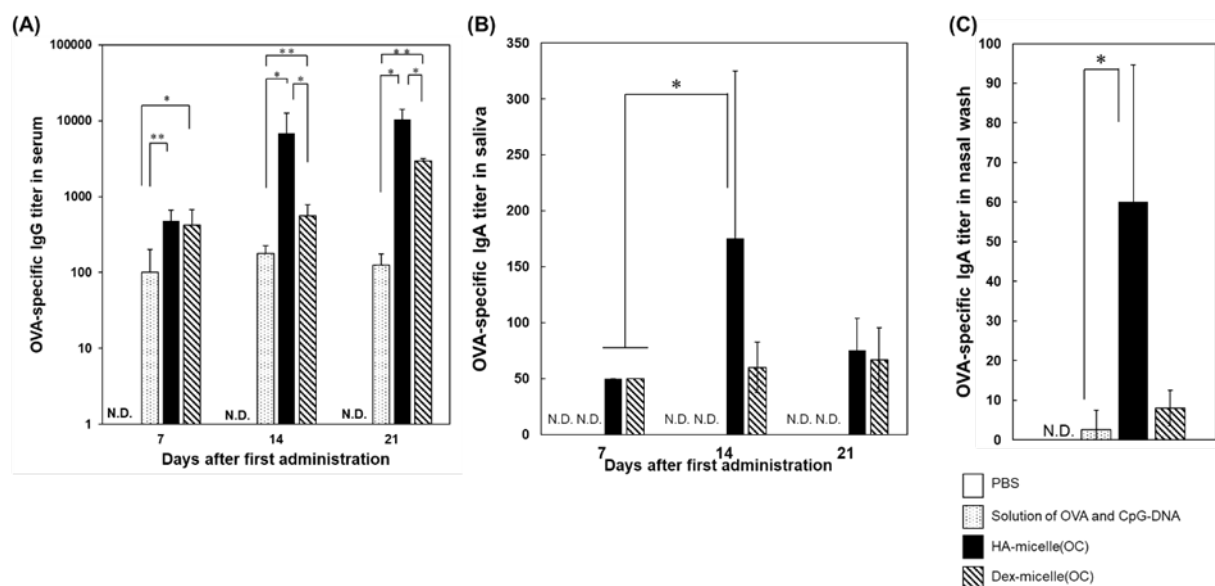


Fig. 7. (A) OVA-specific IgG titers in serum at 7, 14, and 21 days after first nasal administration., (B) OVA-specific IgA titers in saliva at 7, 14, and 21 days after first nasal administration, (C) OVA-specific IgA titers in the nasal wash at 23 days after first nasal administration measured by ELISA for HA-micelle(OC), Dex-micelle(OC), solution of OVA and CpG-DNA, or PBS. * $P < 0.05$, P -value was calculated with Student's t -test. The mice were immunised three times in total at intervals of 7 days. The OVA and CpG-DNA administered per mouse were 10 μg and 2 μg , respectively. Data represent mean \pm SD ($n = 3$ –5). * $P < 0.05$, ** $P < 0.01$.

Fig. 7(A) presents OVA-specific IgG antibody titers in the serum. The OVA-specific IgG antibody titer increased 14, 17, and 21 days after HA-micelle(OC) administration. The mice that received a solution of OVA and CpG-DNA or Dex-micelle(OC) showed increases in OVA-specific IgG levels compared with the PBS-treated group. However, the OVA-specific IgG titer values at 14 and 21 days after the first nasal administration of HA-micelle(OC) were significantly higher than those of solution of OVA and CpG-DNA, or Dex-micelle(OC). These results indicate that humoral immunity could be efficiently induced in mice that received HA-micelle(OC). From these results, it can be concluded that HA-coated micelles are able to pass through the nasal mucosa and activate antigen-presenting cells (mucosa-resident dendritic cells and macrophages).

We also investigated OVA-specific IgA levels in the saliva (Fig. 7(B)). HA-micelle(OC) or Dex-micelle(OC) showed a certain level of OVA-specific IgA titers in saliva at 7, 14, and 21 days after the first administration. However, PBS and the solution of OVA and CpG-DNA did not result in the same effect. On day 14, HA-micelle(OC) showed a higher OVA-specific IgA titer than Dex-micelle(OC) (the difference was not statistically significant due to the large error bars; $P < 0.096$ by Student's t -test). No significant difference between HA-micelle(OC) and Dex-micelle(OC) was observed on day 21. These results suggest that nanoparticles coated with anionic polysaccharides can pass through the nasal mucosa and increase the antibody titer in the mucosa, apart from the administration site. The efficacy of antigen and adjuvant delivery and activation to/of

immunocompetent cells for HA-micelle(OC) were similar or higher than those for Dex-micelle(OC).

OVA-specific IgA levels in the nasal wash were also investigated (Fig. 7(C)). The IgA titers in the nasal wash on day 21 were significantly increased by HA-micelle(OC) administration compared to the normal level (PBS) and the group that received OVA and CpG-DNA. HA-micelle(OC) showed a higher OVA-specific IgA titer in the nasal wash than Dex-micelle(OC), but the difference was not statistically significant ($P < 0.067$ by Student's t -test). This tendency was similar to the results for the titer in saliva.

As the number of antibodies in the saliva and nasal discharge is small, the results cannot be conclusive. However, by loading nanoparticles coated with anionic polysaccharides, mucosal adsorption and absorption of the antibody (OVA) and adjuvant (CpG-DNA) from the nasal mucosa were increased compared to the case of solution administration, leading to the growth of OVA-specific IgA levels in the mucous membrane. This tendency is more significant when HA-micelle(OC) are used, confirming the positive contribution of specific uptake into mucosal epithelial cells with HA receptors.

Conclusions

In this study, we developed an intranasal vaccine delivery system using polymeric micelles coated with hyaluronic acid *via* PIC formation (HA-coated micelles). Micelles were prepared using a block copolymer, P(Lys⁺-*b*-PLA), and HA coating. HA-coated micelles efficiently entrapped the antigen (OVA) and

oligonucleotide adjuvant (CpG-DNA) into the micelles by electrostatic interactions. HA-coated micelles efficiently delivered the antigen and the adjuvant to mouse bone marrow-derived dendritic cells (BMDCs) *in vitro* and strongly activated BMDCs. Intranasal administration of HA-coated micelles to mice significantly increased antigen-specific IgG levels in the blood and IgA levels in the nasal lavage fluid. The results suggested that HA coating enhanced nasal mucosal permeability and retention. Therefore, HA-coated micelles represent a promising platform for developing intranasal vaccine delivery systems.

Experimental

Materials

The diblock copolymer PLys⁺-*b*-PLLA was prepared as reported previously³⁶. The synthetic procedures and the characterisation were described in ESI (Figs. S1-3). Hyaluronic acid sodium salt (HA/Na, Mw = ~90,000 Da) was obtained from Kibun Food Chemifa Co., Ltd. (Tokyo, Japan). CM-Dex sodium salt (Mw = ~40,000 Da) was purchased from Tokyo Chemical Industry Co., Ltd. (Tokyo, Japan). Albumin from chicken egg white (OVA), rhodamine B isothiocyanate (RITC) (mixed isomers), Triton X-100, and 2,2'-azino-bis(3-ethylbenzothiazoline-6-sulfonate) were purchased from Sigma-Aldrich Co. LLC (St. Louis, MO, USA). CpG-DNA and FAM-labelled CpG-DNA were purchased from GeneDesign Inc. (Ibaraki, Japan). Fetal bovine serum (FBS) was purchased from BioWest (Nuaille, France). Granulocyte macrophage colony-stimulating factor (GM-CSF) was purchased from PeproTech Inc. (Cranbury, NJ, USA). Pilocarpine hydrochloride and RPMI-1640 were purchased from Nacalai Tesque, Inc. (Kyoto, Japan). Goat pAb to Ms IgG and IgA (HRP) were obtained from Abcam, Inc. (Cambridge, UK). CD16/32 antibody, phycoerythrin (PE)-labelled anti-CD11c antibody, and PE-labelled anti-MHC class II antibody were purchased from Thermo Fischer Scientific (Waltham, MA, USA). The peroxidase colour development kit was purchased from Sumitomo Bakelite Co. Ltd. (Japan). Murine IFN- γ and IL-4 ABTS ELISA development kits were purchased from Funakoshi Co., Ltd. (Tokyo, Japan). NucleoSpinTM RNA and the PrimeScriptTM RT Reagent Kit were obtained from Takara Bio Inc. (Shiga, Japan). The SsoAdvanced Universal SYBR Green Supermix was purchased from Bio-Rad Laboratories, Inc. (Hercules, CA, USA). Primers for RT-qPCR were obtained from Eurofin Genomics LLC (Louisville, KY, USA), and the sequences of primers are shown in Table S1. Dulbecco's phosphate-buffered saline (PBS(-)) and L-glutamine were purchased from Nissui Pharmaceutical Co., Ltd. (Tokyo, Japan). Ethylenediamine-*N,N,N',N'*-tetraacetic acid (EDTA-2Na) was purchased from Dojindo Laboratories Co., Ltd. (Kumamoto, Japan). Water was purified using Millipore Elix UV3 direct-Q UV (Merck, Darmstadt, Germany).

Measurements

DLS measurements was performed using a Zetasizer Nano Z ZEN 2600 (Malvern Instruments, Ltd., Malvern, UK). TEM was performed using a transmission electron microscope (JEOL JEM-1210, Tokyo, Japan). Before observation, one drop of the micelle solution in pure water was placed on a carbon-coated copper grid, dried in the air,

and negatively stained with a 3 wt% ammonium molybdate aqueous solution. The fluorescence spectra were recorded using an FP-8300 fluorescence spectrophotometer (JASCO Corp. Tokyo, Japan). Fluorescence microscopy images were recorded on a CLSM (LSM 800 Axio Observer.Z1, Carl Zeiss AG, Oberkochen, Germany) using diode lasers at 488 and 561 nm. FCA was performed using a Gallios flow cytometer (Beckman Coulter, Inc., Brea, CA, USA) with an argon-ion coherent beam laser (488 nm).

Preparation of PLys⁺-*b*-PLLA micelles

PLys⁺-*b*-PLLA micelles were prepared as reported previously³⁶. PLys⁺-*b*-PLLA (22.1 mg) was dissolved in THF (3 mL) and added dropwise to a large volume of pure water under stirring. After stirring for 20 min, the mixture was sonicated. The organic solvent was then removed using an evaporator. Polymeric micelles were obtained as a white solid by freeze-drying (yield: 93%).

Preparation of hyaluronic acid (HA)-coated micelles containing OVA and CpG-DNA

HA-coated micelles containing rhodamine B-labelled OVA and FAM-labelled CpG-DNA (HA-micelle(OC)) were prepared according to a previously reported method with modification³⁶. OVA was labelled with rhodamine B using RITC. OVA (102 mg) and RITC (5 mg) were dissolved in 0.5 M NaHCO₃ buffer (pH = 9.0, 10 mL), and the solution was stirred at 4°C for 24 h. The product was dialysed (molecular weight cutoff [MWCO] = 10,000 g/mol) in the dark for 72 h, followed by lyophilisation. PLys⁺-*b*-PLLA micelles (1.2 mg), rhodamine B-labelled OVA (0.52 mg), and FAM-labelled CpG-DNA (0.0522 mg) were dissolved in ultrapure water (1 mL), respectively. Meanwhile, HA/Na (2.9 mg) was also dissolved in ultrapure water (0.5 mg/mL). An aqueous solution of rhodamine B-labelled OVA and FAM-labelled CpG-DNA was slowly added dropwise to the PLys⁺-*b*-PLLA micelle solution, and the mixture was stirred for 20 min. The HA/Na solution was then slowly added dropwise to the reaction mixture under stirring, and the total anion/cation ratio was 1.4/1. After stirring for 20 min, centrifugation was performed at 1,500 rpm for 10 min using an ultrafiltration membrane (MWCO = 300,000 g/mol). After lyophilisation of the supernatant, HA-micelle(OC) were obtained as a white solid (yield: 84%). CM-Dex-coated micelles containing rhodamine B-labelled OVA and FAM-labelled CpG-DNA (Dex-micelle(OC)) were also prepared using the same method (yield: 85%). For estimating the amount of entrapped OVA and CpG-DNA, HA-micelle(OC) or Dex-micelle(OC) were stirred in a 30% phosphate-buffered solution of Triton X-100 for 20 min to collapse micelles. The entrapment amounts of OVA and CpG-DNA were calculated using the calibration curve of rhodamine B-labelled OVA and FAM-labelled CpG-DNA. HA-micelle(OC) and Dex-micelle(OC) containing non-labelled-OVA and CpG-DNA were also prepared by the same method and used for determination of MHC class II molecules expression on BMDCs and *in vivo* experiments.

Animals

C57BL/6N mice (6-week-old, female) were purchased from SHIMIZU Laboratory Supplies Co., Ltd. (Kyoto, Japan). The experiments were performed under the influence of anaesthesia gas (isoflurane) using a small animal anaesthesia station (DS Pharma Biomedical Co., Ltd. Osaka, Japan). The animal experiments described below were performed following the guidelines for animal experiments listed at Kansai University and were approved by the Ethical Committee for

Animal Experiments of Kansai University (7 May 2019 Identification No.1903).

Bone marrow-derived dendritic cells (BMDCs)

Bones were collected from the hind limbs of C57BL6/N mice, soaked in ethanol for 5 s, and washed with R10 medium (RPMI-1640 supplemented with 10% FBS, 50 μ M 2-mercaptoethanol, 100 U/mL penicillin, 100 μ g/mL streptomycin). R10 medium (1 mL) was injected into the cut bone, and bone marrow cells were collected in a centrifuge tube. Subsequently, the cell suspension was centrifuged for 5 min at 1200 rpm, and R10 (3 mL) was added. Cell counting was performed using a hemocytometer. The cell suspension was cryopreserved in CELLBANKER1 (TaKaRa Bio, Inc.).

The BMDCs were generated according to a previously reported³⁸. Bone marrow cells were seeded in a non-adhesive petri dish (10 cm) at 2 million cells/well, medium for BMDC (R10 medium containing 10 ng/mL GM-CSF) was added, and the cells were incubated in an incubator 5% CO₂ atmosphere at 37°C on day 0. The medium containing cells (10 mL) was collected and centrifuged to remove the supernatant, and a fresh medium for BMDC (10 mL) was added on days 3 and 5. After 7 days of culture, non-adherent and weakly adherent cells were collected as BMDCs.

Quantification of dendritic cell marker (CD11c⁺) was performed as follows: BMDCs were adjusted to 1 million cells/tube, and CD16/32 antibody was added. The mixture was incubated on ice for 30 min to block non-specific adsorption. Next, a PE-labelled CD11c antibody was added, and incubation on ice continued for another 30 min. In each step, cells were washed thrice with staining buffer. Finally, the fluorescence intensity of BMDCs was measured using a flow cytometer (Gallios, Beckman Coulter, Inc., Brea, CA, USA). The results are shown in the ESI (Fig. S4).

Uptake of HA-coated micelles into BMDC

BMDCs were seeded on glass-bottom dishes at 1×10^5 cells/well density and incubated at 37°C for 48 h. After removing the medium, the cells were washed with PBS(-). Then, medium and the same volume of an aqueous solution of HA-micelle(OC) (3 mg/mL) were added (final micelle concentration = 1.5 mg/mL), and the mixture was incubated at 37°C for 4 h. After washing with PBS(-), the uptake behaviour of the HA-micelle(OC) in the cells was monitored using CLSM or FCM. Solutions of Dex-micelle(OC) were used as controls.

Quantification of mRNA in BMDCs

BMDCs (5×10^4 cells) were seeded on a glass-bottom dish and pre-incubated at 37°C for 48 h. A solution of HA-micelle(OC) containing OVA (26 μ g) and CpG-DNA (2.6 μ g) (final concentration = 1.5 mg/mL) was added to the well, and the mixture was incubated. After 24 h, the cells were washed with PBS(-). mRNA extraction and RT-qPCR were performed using NucleoSpin RNA and PrimeScrip RT reagent, respectively, according to the instruction provided by the manufacturer. The mRNA levels of IL-4 and IFN- γ were quantified using a Bio-Rad CFX96 Deep well Real-Time System (Bio-Rad Laboratories Inc., Hercules, CA, USA), SsoAdvanced Universal SYBR Green Supermix, and primers obtained from Eurofin Genomics LLC (Louisville, KY, USA) (Table S1). The relative mRNA expression of IL-4 and IFN- γ was determined using the formula $Rel\ Exp = 2^{-\Delta Ct}$, where $\Delta Ct = Ct_{\text{gene of interest}} - Ct_{\beta\text{-actin}}$ in experimental samples. Equivalent amounts of OVA (26 μ g) and CpG-DNA (2.6 μ g) dissolved in PBS(-) were used as controls.

Evaluation of expression of MHC class II molecules on BMDCs

BMDCs (1.5×10^5 cells in 25 μ L) were incubated with HA-micelle(OC) containing OVA (10 μ g) and CpG-DNA (1 μ g) on a glass-bottom dish at 37°C for 24 h and collected in an Eppendorf tube. Anti-CD16/32 antibody (0.075 μ g/100 μ L) was added to the BMDCs to suppress non-specific adsorption of the antibody and incubated in an ice bath for 30 min. After the addition of PE-labelled anti-MHC class II antibody to BMDCs, Eppendorf tubes were incubated in an ice bath for 30 min. The fluorescence intensity of the cells was measured using a flow cytometer at 575 nm (excitation, 488 nm). A mixed solution of OVA (10 μ g) and CpG-DNA (1 μ g; 25 μ L) was used as a control.

Trans-nasal administration of vaccines to mice and immunological evaluation of serum and saliva

Each sample, HA-micelle(OC) (number of mice (n) = 5), Dex-micelle(OC) (n = 5), solution of OVA and CpG-DNA (n = 4), and PBS(-) (n = 3), was administered to mice *via* the nasal route three times at 7 days intervals (total OVA amount = 10 μ g, total amount of CpG-DNA = 2 μ g, solution: 20 μ L \times 3 times/mouse). The serum and saliva of each mouse were collected at 7 days intervals after the first administration. After anaesthetising the mice under 2% isoflurane, the tail vein was slightly cut with a gym knife, and blood (100 μ L) was collected. After incubation at 37°C for 1 h, blood clots were removed. After centrifugation (3000 g, 30 min, 4°C), serum was collected and stored at -30°C until use. Mouse saliva was collected according to previously reported methods, with slight modification³⁸. After anaesthetising with 2% isoflurane, the mice received an intraperitoneal injection of pilocarpine hydrochloride in PBS(-) (0.25 mg/mL) (0.1 mL/mouse). After approximately 4 min, saliva was collected with a micropipette and stored at -30°C until use. OVA-specific IgG antibody titration was performed using ELISA, as previously reported³⁹.

Statistical analysis

Data are expressed as mean \pm standard deviation (SD) and were analysed using the bell-curve statistical analysis software in Microsoft Excel (Tokyo, Japan). Significant differences between the mean values of the two groups were evaluated using the Student's *t*-test. Statistical significance was set at $P < 0.05$.

Acknowledgments

This work was financially supported in part by the Private University Research Branding Project: Matching Fund Subsidy from the Ministry of Education, Culture, Sports, Science, and Technology (MEXT) Japan (2016–2020), Grants-in-Aid for Scientific Research (20H00670) from the Japan Society for the Promotion of Science (JSPS), and Kansai University Contingency Fund for Education and Research Outlay (2020).

Author Contributions

YO and YY conceived the idea, designed the experiments and analysed the data. KS performed all of the experiments including the synthesis of the material. KH performed some of the *in vitro* and *in vivo* experiments. NM and AK analysed the results. The manuscript was prepared by YO, YY and MN. All authors discussed the results.

Conflicts of interest

There are no conflicts to declare.

Notes and references

- J. R. Teijaro and D. L. Farber, *Nat. Rev. Immunol.*, 2021, **21**, 195-197.
- E. Bettini, M. Locci, *Vaccines*, 2021, **9**, 147.
- A. J. Macpherson, M. B. Geuking and K. D. McCoy, *Trends Immunol.*, 2012, **33**, 160-167.
- S. Al-Halifa, L. Gauthier, D. Arpin, S. Bourgault and D. Archambault, *Front. Immunol.*, 2019, **10**, 22.
- B. Bernocchi, R. Carpentier and D. Betbeder, *Int. J. Pharm.*, 2017, **530**, 128-138.
- A. R. Khan, M. R. Liu, M. W. Khan and G. X. Zhai, *J. Control Release*, 2017, **268**, 364-389.
- A. C. Anselmo, Y. Gokarn and S. Mitragotri, *Nat. Rev. Drug Discov.*, 2019, **18**, 19-40.
- L. Illum, *J. Control Release*, 2003, **87**, 187-198.
- S. Mitragotri, *Nat. Rev. Immunol.*, 2005, **5**, 905-916.
- H. Hasegawa, S. Kadowaki, H. Takahashi, T. Iwasaki, S. Tamura and T. Kurata, *Vaccine*, 2000, **18**, 2560-2565.
- S. N. Georas and F. Rezaee, *J. Allergy. Clin. Immunol.*, 2014, **134**, 509-520.
- S. Y. Chang, H. Y. Ko and M. N. Kweon, *Exp. Mol. Med.*, 2014, **46**, e84.
- S. Singha, K. Shao, K. K. Ellestad, Y. Yang and P. Santamaria, *ACS Nano*, 2018, **12**, 10621-10635.
- M. R. Neutra and P. A. Kozlowski, *Nat. Rev. Immunol.*, 2006, **6**, 148-158.
- A. J. Almeida and E. Souto, *Adv. Drug. Deliv. Rev.*, 2007, **59**, 478-490.
- L. J. Peek, C. R. Middaugh and C. Berkland, *Adv. Drug. Deliv. Rev.*, 2008, **60**, 915-928.
- C. A. Garcia-Gonzalez, A. Sosnik, J. Kalmar, I. De Marco, C. Erkey, A. Concheiro and C. Alvarez-Lorenzo, *J. Control Release*, 2021, **332**, 40-63.
- J. D. Pachioni-Vasconcelos, A. M. Lopes, A. C. Apolinario, J. K. Valenzuela-Oses, J. S. R. Costa, L. D. Nascimento, A. Pessoa, L. R. S. Barbosa and C. D. Rangel-Yagui, *Biomater. Sci.*, 2016, **4**, 205-218.
- P. M. Lackie, J. E. Baker, U. Günthert and S. T. Holgate, *Am. J. Respir. Cell. Mol. Biol.*, 1997, **16**, 14-22.
- A. Mero and M. Campisi, *Polymers*, 2014, **6**, 346-369.
- D. H. Jiang, J. R. Liang and P. W. Noble, *Physiol. Rev.*, 2011, **91**, 221-264.
- R. J. Verheul, B. Slutter, S. M. Bal, J. A. Bouwstra, W. Jiskoot and W. E. Hennink, *J. Control. Release*, 2011, **156**, 46-52.
- L. X. Liu, F. Q. Cao, X. X. Liu, H. Wang, C. Zhang, H. F. Sun, C. Wang, X. G. Leng, C. X. Song, D. L. Kong and G. L. Ma, *Appl. Mater. Interfaces*, 2016, **8**, 11969-11979.
- L. Illum, N. F. Farraj, A. N. Fisher, I. Gill, M. Miglietta and L. M. Benedetti, *J. Control. Release*, 1994, **29**, 133-141.
- M. Singh, M. Briones and D. T. O'Hagan, *J. Control. Release*, 2001, **70**, 267-276.
- Y. C. Fan, P. Sahdev, L. J. Ochyl, J. J. Akerberg and J. J. Moon, *J. Control. Release*, 2015, **208**, 121-129.
- K. Pritchard, A. B. Lansley, G. P. Martin, M. Helliwell, C. Marriott and L. M. Benedetti, *Int. J. Pharm.*, 1996, **129**, 137-145.
- K. Kataoka, A. Harada and Y. Nagasaki, *Adv. Drug. Deliv. Rev.*, 2001, **47**, 113-131.
- H. Cabral, K. Miyata, K. Osada and K. Kataoka, *Chem. Rev.*, 2018, **118**, 6844-6892.
- A. Mandal, R. Bisht, I. D. Rupenthal and A. K. Mitra, *J. Control Release*, 2017, **248**, 96-116.
- S. H. S. Leung and J. R. Robinson, *J. Control Release*, 1987, **5**, 223-231.
- R. Sharma, U. Agrawal, N. Mody and S. P. Vyas, *Biotechnol. Adv.*, 2015, **33**, 64-79.
- W. J. Fan, L. Liu and H. Y. Zhao, *Angew. Chem. Int. Ed.*, 2017, **56**, 8844-8848.
- H. S. Min, H. J. Kim, J. Ahn, M. Naito, K. Hayashi, K. Toh, B.S. Kim, Y. Matsumura, I. C. Kwon, K. Miyata and K. Kataoka, *Biomacromolecules*, 2018, **19**, 2320-2329.
- Y. T. Wang, L. P. Huang, Y. Shen, L. D. Tang, R. N. Sun, D. Shi, T. J. Webster, J. S. Tu and C. M. Sun, *Int. J. Nanomedicine*, 2017, **12**, 7963-7977.
- Y. Ohya, S. Takeda, Y. Shibata, T. Ouchi and A. Maruyama, *Macromol. Chem. Phys.*, 2010, **211**, 1750-1756.
- Y. Ohya, S. Takeda, Y. Shibata, T. Ouchi, A. Kano, T. Iwata, S. Mochizuki, Y. Taniwaki and A. Maruyama, *J. Control. Release*, 2011, **155**, 104-110.
- M. J. McCluskie, R. D. Weeratna and H. L. Davis, *Mol. Med.*, 2000, **6**, 867-877.
- E. Yuba, A. Harada, Y. Sakanishi, S. Watarai and K. Kono, *Biomaterials*, 2013, **34**, 3042-3052.
- Y. Yoshizaki, E. Yuba, N. Sakaguchi, K. Koiwai, A. Harada and K. Kono, *Biomaterials*, 2017, **141**, 272-283.
- J. J. Varghese, I. L. Schmale, M. E. Hansen, S. D. Newlands, D. S. W. Benoit and C. E. Ovitt, *J. Vis. Exp.*, 2018, **135**, e57522.